

# Formation of Supported Lipid Bilayers by Vesicle Fusion: Effect of Deposition Temperature

Tania Kjellerup Lind,<sup>\*,†,‡</sup> Marité Cárdenas,<sup>\*,†,§</sup> and Hanna Pauliina Wacklin<sup>†,‡</sup>

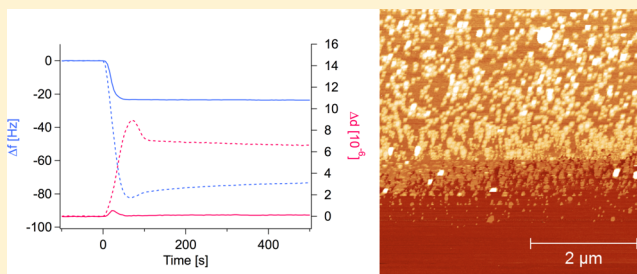
<sup>†</sup>Nano-Science Center and Institute of Chemistry, Copenhagen University, Copenhagen, Denmark

<sup>‡</sup>European Spallation Source ESS AB, Lund, Sweden

<sup>§</sup>Malmö University, Health & Society, 20506 Malmö, Sweden

## S Supporting Information

**ABSTRACT:** We have investigated the effect of deposition temperature on supported lipid bilayer formation via vesicle fusion. By using several complementary surface-sensitive techniques, we demonstrate that despite contradicting literature on the subject, high-quality bilayers can be formed below the main phase-transition temperature of the lipid. We have carefully studied the formation mechanism of supported DPPC bilayers below and above the lipid melting temperature ( $T_m$ ) by quartz crystal microbalance and atomic force microscopy under continuous flow conditions. We also measured the structure of lipid bilayers formed below or above  $T_m$  by neutron reflection and investigated the effect of subsequent cooling to below the  $T_m$ . Our results clearly show that a continuous supported bilayer can be formed with high surface coverage below the lipid  $T_m$ . We also demonstrate that the high dissipation responses observed during the deposition process by QCM-D correspond to vesicles absorbed on top of a continuous bilayer and not to a surface-supported vesicular layer as previously reported.



## INTRODUCTION

Supported lipid bilayers (SLBs) are commonly used as simple model systems for cell membranes,<sup>1</sup> for instance, to study enzymatic lipolysis<sup>2</sup> or to understand the binding mechanisms of antibacterial drugs.<sup>3,4</sup> They can be formed by several methods, including vesicle fusion,<sup>5</sup> the lipid-detergent method,<sup>6,7</sup> and Langmuir–Blodgett deposition.<sup>8</sup> The physicochemical properties in terms of lipid composition, leaflet asymmetry, in-plane structure, mobility, and fluidity have been studied extensively by a range of techniques including atomic force microscopy (AFM),<sup>9–11</sup> dissipation-enhanced quartz crystal microbalance (QCM-D),<sup>9–12</sup> ellipsometry,<sup>9</sup> neutron reflection,<sup>11–13</sup> fluorescence microscopy,<sup>11,14</sup> and interferometric scattering microscopy.<sup>15</sup> A key parameter for SLB formation by vesicle fusion is thought to be the deposition temperature, especially for lipids that are in the gel phase at room temperature.<sup>16</sup> In many cases, contradictory information about SLB formation (e.g., *E. coli* bacterial lipids) exists in the literature. This seems to be coupled to the type of method used for the evaluation of SLB formation.<sup>17–20</sup> We present a detailed study of the effect of deposition temperature on the quality of SLBs formed by DPPC. We have used three different surface-sensitive techniques: QCM-D, neutron reflection, and AFM under continuous flow conditions.<sup>4</sup> QCM-D gives an estimate of the wet adsorbed mass, and it is thus particularly sensitive to the presence of water-filled vesicles, whether they are attached to the sensor surface as a supported vesicle layer or coadsorbed in defects in a bilayer or on top of it. This

technique is commonly used to assess the quality of SLBs and the success of various protocols for SLB formation.<sup>21</sup> Neutron reflection, on the other hand, gives detailed information on the structure and composition of the SLB in a direction perpendicular to the interface, but it is not particularly sensitive to the presence of a small number of vesicles, as they have a low scattering contrast with respect to the surrounding solution. AFM gives complementary information about the lateral organization of the lipid bilayers and allows for real-time imaging of bilayer formation under continuous flow conditions.<sup>4</sup> In this letter, we show that a combination of these three techniques is essential for a complete understanding of the structure and formation mechanism of SLBs.

## EXPERIMENTAL SECTION

**Materials.** 1,2-Dipalmitoyl-*sn*-glycero-3-phosphocholine (DPPC) was purchased from Avanti Polar Lipids, Inc. (Alabaster, AL). D<sub>2</sub>O was provided by the Institut Laue-Langevin, Grenoble, France, or purchased from Sigma-Aldrich Inc. Ultrapure Milli-Q water with a resistivity of 18.2 MΩ·cm (Thermo Scientific, Branstead Nanopure 7145) was used for all cleaning procedures and sample preparation methods. Hellmanex 2% (Hellma GmbH & Co, Germany) and absolute ethanol were used to clean QCM-D sensor crystals (purchased from QSense, Biolin Scientific, Stockholm, Sweden). Chloroform was purchased from Sigma-Aldrich Inc.

**Received:** March 6, 2014

**Revised:** June 7, 2014

**Published:** June 16, 2014

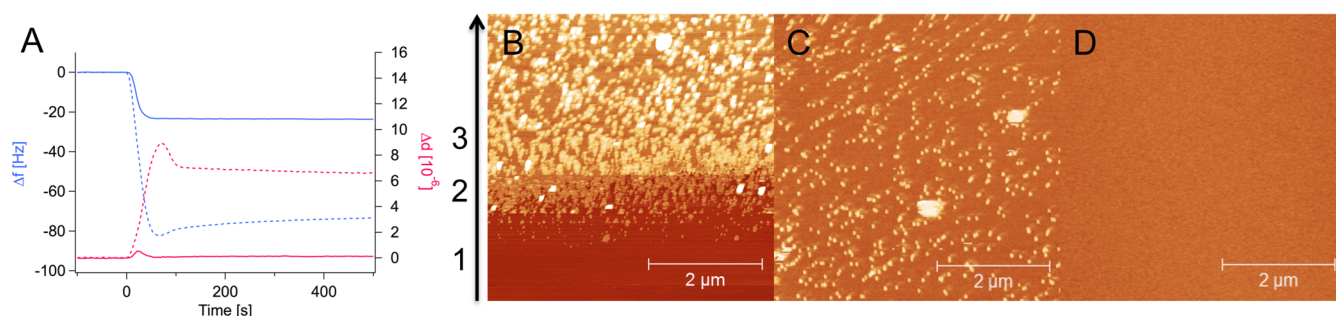


**Figure 1.** (A)  $\Delta f$  (blue) and  $\Delta d$  (red) as a function of vesicle exposure time on a clean silica surface at 25 °C (broken lines) or 50 °C (solid lines). The data shown corresponds to the seventh overtone. At  $t = 0$  s, a solution of SUVs was introduced into the cells. (B) AFM image of the formation of a DPPC bilayer at RT under constant flow conditions. Raster scanning was performed in the direction along the arrow. The numbers correspond to (1) clean mica, before lipids have reached the surface, (2) small lipid bilayer patches formed instantaneously and fused to create a bilayer, and (3) vesicles attached to the bilayer. (C) Imaging during rinsing with water at RT. (D) Image after rinsing and equilibration with hot water (above  $T_m$ ).

**Small Unilamellar Vesicles (SUVs).** These were prepared by tip sonication of lipid films hydrated in ultrapure water above the lipid  $T_m$  (42 °C) and then kept in the fluid phase or at room temperature, as described earlier.<sup>4,11</sup>

**Quartz Crystal Microbalance.** Quartz crystal microbalance with dissipation was performed with the Q-SENSE E4 system (QSense, Biolin Scientific, Stockholm, Sweden). Silicon oxide sensors, 50 nm, were purchased from QSense, and cleaning was performed as earlier described.<sup>4,11</sup> The fundamental frequency and six overtones were recorded during lipid bilayer formation at either 50 or 25 °C. SUVs in ultrapure water, at a concentration of 250  $\mu\text{g/mL}$ , were injected into the cells using a peristaltic pump (Ismatec IPC-N 4) at 100  $\mu\text{L/min}$ . After successful bilayer formation, the membranes were rinsed with ultrapure water followed by phosphate-buffered saline (PBS, 10 mM, NaCl 100 mM, pH 7.4) before lowering the temperature to 25 °C (in cases of deposition at 50 °C). Bilayer formation above the  $T_m$  was very reproducible in the QCM. We found a standard deviation of 2.5% in mass adsorption between different depositions (nineteen depositions in eleven different experiments). Deposition at 25 °C was less reproducible as the adsorbed mass depends on the number and size of the attached vesicles, which is strongly influenced by factors such as the equilibration time, the size distribution, the buffer conditions, and so forth. Thirteen depositions (in four different experiments) of DPPC at RT in pure water were performed, and we found a standard deviation between depositions of 14.5%.

**Atomic Force Microscopy.** Atomic force microscopy measurements were carried out on a Nanoscope IV multimode AFM (Veeco Instruments Inc.). Images were generated in the PeakForce QNM (quantitative nanomechanical property mapping) mode with a silicon oxide tip (Olympus microcantilever OTR8 PS-W) having a spring constant of 0.15 N/m and a radius of curvature of <20 nm. Continuous-flow AFM imaging was done at room temperature ( $\sim 25$  °C) as described previously<sup>4</sup> using a slow gravity-fed flow of 40–50  $\mu\text{L/min}$  to minimize turbulence around the cantilever. After bilayer formation in ultrapure water, the membranes were rinsed with PBS. All images were recorded at a resolution of  $512 \times 512$  pixels and with a scan rate of 1 Hz. The z-set point and differential gains were manually optimized during each scan. Images were analyzed and processed in the Gwyddion 2.22 software. Deposition in the AFM was performed twice and showed bilayers of high coverage with attached vesicles.

**Neutron Reflection (NR).** Neutron reflection measurements were performed using homemade flow cells. Silicon (111) surfaces were cleaned for 15 min in 5:4:1  $\text{H}_2\text{O}/\text{H}_2\text{SO}_4/\text{H}_2\text{O}_2$  at 80 °C before each experiment. Reflectometers FIGARO<sup>22</sup> and D17<sup>23</sup> at Institute Laue-Langevin (Grenoble, France) and INTER (ISIS, Didcot, U.K.) were used to record the time-of-flight reflectivity at two angles of incidence (FIGARO, 0.624 and 3.78°; D17, 0.8 and 3.2°; INTER, 0.7 and 2.3°). The temperature was controlled using a water bath at either 25 or 50 °C. The vesicles were equilibrated in the cell for  $\sim 1$  h before rinsing with PBS. Then the temperature was decreased to 25 °C, and the bilayers were characterized using at least two water contrasts ( $\text{D}_2\text{O}$ ,

$\text{H}_2\text{O}$ , and their mixtures). All NR profiles were analyzed as described previously<sup>11–13,24</sup> using the Motofit package,<sup>25</sup> which uses the Abeles optical matrix method to calculate the reflectivity of thin layers. Two experiments were carried out below the lipid  $T_m$  and varied by 5% or less in coverage and thickness of the different layers. For deposition at 50 °C, the deviation between three different experiments was 14% in coverage, 10% in headgroup thickness, and 3% in total tail thickness.<sup>11,24</sup>

## RESULTS AND DISCUSSION

Figure 1A shows the QCM-D signals from vesicle deposition above (50 °C) or below (25 °C) the lipid  $T_m$ . For deposition above the lipid  $T_m$  (solid lines), the bilayer formation proceeded with the characteristic frequency and dissipation changes corresponding to vesicle adsorption, fusion, and spreading of the lipids to form a continuous bilayer.<sup>5,21</sup> In this case, no distinct frequency minimum was observed, which indicated that the vesicles spread on contact with the surface, without the buildup of a critical surface coverage of vesicles before rupture and fusion. This is highly dependent on the solution conditions used. Figure S1 in the Supporting Information shows QCM-D traces of DPPC deposition in PBS buffer versus pure water at 25 and 50 °C. A frequency change of  $-25$  Hz corresponds to a typical full bilayer coverage, and a dissipation change below  $1 \times 10^{-6}$  indicates a thin and rigid layer.<sup>26</sup> However, significantly higher frequency and dissipation changes were observed for deposition at 25 °C. This is often interpreted as unsuccessful SLB formation when vesicles remain attached to the surface without fusing, the so-called supported vesicular layer or only partially fused vesicles.<sup>10</sup> QCM-D is highly sensitive to water-filled vesicles, and thus  $\Delta f$  and  $\Delta d$  responses related to fusion and bilayer formation cannot be separated if vesicles are simultaneously adsorbed on top of the forming bilayer. Therefore, whether or not a bilayer is formed cannot necessarily be resolved only from QCM-D data.

Figure 1B shows in situ AFM images obtained under constant flow conditions<sup>4</sup> to visualize the initial stages of vesicle adsorption, fusion, and bilayer formation. As the lipid solution reached the mica surface, the vesicles spontaneously fused to form small patches of bilayer (Figure 1B, no. 1), which readily spread to form a continuous bilayer (Figure 1B, no. 2). As the bilayer formed, lipid vesicles attached to the top of it and remained intact (Figure 1B, no. 3). Slow rinsing with water at room temperature removed some of the attached vesicles (Figure 1C). To remove all of the vesicles, it was necessary to rinse quickly with preheated water above the lipid  $T_m$  (Figure

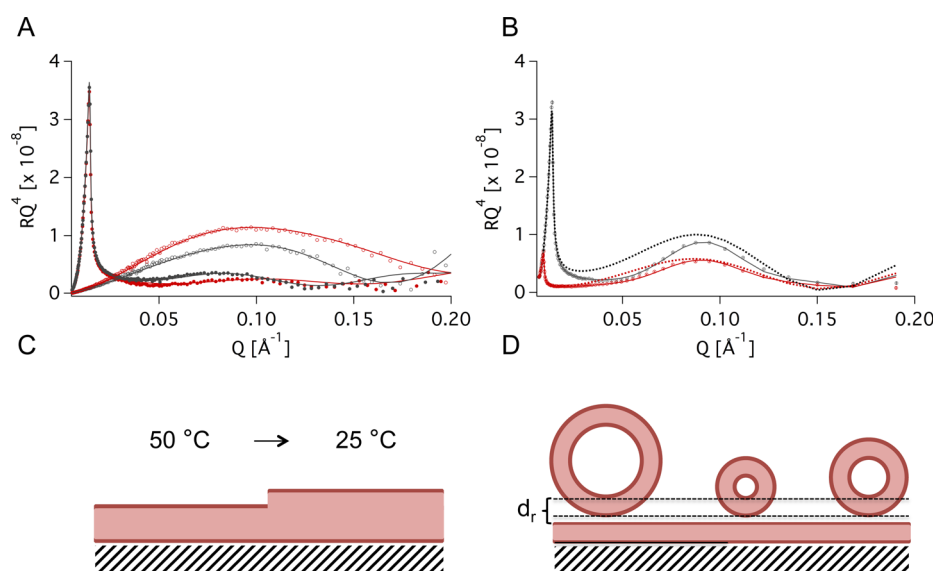


**Figure 2.** Neutron reflectivity curves. (A) dPPC measured at 50 °C (red) and after cooling to 25 °C (gray). Data points in solid circles were measured in D<sub>2</sub>O (SLD =  $6.35 \times 10^{-6} \text{ Å}^{-2}$ ), while data points in open circles were measured in H<sub>2</sub>O (SLD =  $-0.56 \times 10^{-6} \text{ Å}^{-2}$ ). (B) hDPPC membrane deposited and measured at 25 °C. The gray data points and the solid line correspond to reflectivity measured in D<sub>2</sub>O and the best fit to the data. This fit includes an additional lipid layer on top of the membrane, separated by a layer of water. The additional layer has a coverage of  $14 \pm 1 \text{ v/v\%}$  and is believed to stem from attached vesicles. The red data is measured in CM4 (contrast matched to SLD =  $4 \times 10^{-6} \text{ Å}^{-2}$ ). The broken lines give the corresponding fits for a model without an additional lipid layer for comparison. Note that the data has been plotted as RQ<sup>4</sup> versus Q in order to highlight the difference between the fits. (C) Model (not to scale) of the effect of cooling the membrane to 25 °C. (D) Model of the membrane including attached vesicles, which would give rise an additional layer aligned with the membrane.  $d_r$  denotes the repeat distance which is consistent with the  $d_r$  of multilamellar vesicles of DPPC (Supporting Information Figure S2). The clean surfaces were measured in D<sub>2</sub>O and H<sub>2</sub>O, but the data and fits have been omitted for clarity in both A and B.

**Table 1.** Parameters Used for the Fits Shown in Figure 2<sup>a</sup>

sample	deposition temp/°C	measured temp/°C	layer	$d/\text{Å}$	$\phi/\%$	$A_{\text{wet}}/\text{Å}^2$	$A_{\text{mol}}/\text{Å}^2$	$\Gamma/\text{mg m}^{-2}$	$d/\text{Å}$
1	50	50	head	6.8	70	$69 \pm 11$	$64 \pm 3$	$3.5 \pm 0.5$	$41.6 \pm 6$
			tail	28	91	$70 \pm 4$			
			head	6.8	70	$69 \pm 11$			
		25	head	6.6	72	$69 \pm 11$	$47 \pm 2$	$3.5 \pm 0.6$	$50.7 \pm 6$
			tail	37.5	68	$70 \pm 4$			
			head	6.6	72	$69 \pm 11$			
2	25	25	head	6.8	86	$55 \pm 8$	$48 \pm 2$	$4.4 \pm 0.7$	$50.1 \pm 6$
			tail	37	87	$55 \pm 4$			
			head	6.8	86	$55 \pm 8$			
			water	14	100		$0.7 \pm 0.3$		$14 \pm 2$
			bilayer	50	14	$347 \pm 126$			$50 \pm 3$

<sup>a</sup>The parameters used for fitting neutron reflectivity data were  $d$  = thickness,  $\phi$  = surface coverage of the layer,  $A_{\text{wet}}$  = wet area per lipid molecule,  $A_{\text{mol}}$  = area per lipid molecule,  $\Gamma$  = surface density. In sample 1, the SiO<sub>2</sub> layer was  $10 \pm 1 \text{ Å}$  thick,  $4 \pm 1 \text{ Å}$  rough, and contained  $12 \pm 1 \text{ v/v\%}$  water (due to porosity) while in sample 2 the numbers were  $6 \pm 1 \text{ Å}$ ,  $5 \pm 1 \text{ Å}$ , and  $0 \text{ v/v\%}$ , respectively. The lipid heads and tails were assumed to have molecular volumes of  $V_{\text{head}} = 326.3 \text{ Å}^3$  and  $V_{\text{tails}} = 889.2 \text{ Å}^3$ , respectively, obtained from molecular dynamics simulations.<sup>28</sup> The fitting errors of the headgroup and tail thicknesses are  $\pm 1 \text{ Å}$ , while the errors in  $\phi$  are  $\pm 3 \text{ v/v\%}$  as determined by the quality of the fits.<sup>24</sup> The molecular scattering length density of the headgroups was  $1.85 \times 10^{-6}$  for both samples while for the tails the values were  $6.89 \times 10^{-6} \text{ Å}^{-2}$  (dDPPC) for sample 1 and  $-0.35 \times 10^{-6} \text{ Å}^{-2}$  for sample 2 (hDPPC). The SLD of the extra layer of hDPPC in sample 2 was fitted to  $0.3 \times 10^{-6} \text{ Å}^{-2}$ , which is an average of the SLDs of the components of a bilayer.

1D). The bilayer thickness could be assessed from the edge of a defect to be  $6.0 \pm 0.2 \text{ nm}$ .

Finally, the bilayer structure was measured using neutron reflection. The results for chain-deuterated DPPC are summarized in Figure 2A and Table 1 (sample 1). At least two isotopic water contrasts were measured to calculate the thickness, area per molecule, and volume fraction of solvent accurately. The membrane was deposited and measured first at 50 °C and subsequently at 25 °C. The change from a fluid to a gel phase was observed as an increase in the lipid bilayer thickness of approximately  $0.9 \pm 0.2 \text{ nm}$ , mainly due to

lengthening of the lipid tails while maintaining the headgroup thickness.

While the wet area per lipid (the area occupied by lipid plus water from hydration and defects) remained unchanged upon decreasing the temperature, the actual area per lipid molecule was significantly reduced from  $64 \pm 3$  to  $47 \pm 2 \text{ Å}^2$ , as the more densely packed gel-phase lipids take up less space than the fluid phase lipids. These molecular areas are consistent with the literature (fluid phase  $A_{\text{mol}} = 64 \text{ Å}^2$ , gel phase (20 °C)  $A_{\text{mol}} = 47.9 \text{ Å}^2$  (50 °C) according to Nagle et al.<sup>27</sup>).



Deposition below the lipid  $T_m$  (25 °C, hDPPC, sample 2) led to bilayer formation with a thickness and area per lipid similar to those of the membrane deposited at 50 °C and subsequently cooled to 25 °C. This implies that the overall membrane structure was independent of the deposition conditions (Figure 2B and Table 1). However, the data for the membrane deposited at 25 °C could not be fitted to a physically meaningful model of a single supported bilayer but required an additional lipid layer of low surface coverage, approximately  $14 \pm 1$  v/v%. The layer was separated from the SLB by a  $14 \pm 2$  Å thick water layer, consistent with the repeat distance of multilamellar DPPC vesicles measured by small-angle X-ray scattering (see Supporting Information Figure S2 for SAXS data). This layer could represent small patches of a double bilayer or a vesicle layer, where the upper bilayer is very diffuse because of the low surface coverage, the size distribution, and the softness of the material. The additional layer was modeled as a single layer of  $50 \pm 3$  Å with the SLD fitted to the average value expected for DPPC,  $(0.3 \pm 0.2) \times 10^{-6}$  Å<sup>-2</sup>. Although this is a simplified model of a vesicular layer, it is clearly necessary for a good fit to the data; a comparison of the fits with (solid lines) and without (broken lines) the second layer is shown in Figure 2B. Schematic representations of the models used for the fits in Figure 1A,B are found in Figure 2C,D, respectively.

It is a general conception that it is necessary to work above the lipid main transition in order to succeed in supported bilayer deposition by vesicle fusion. Indeed, there are few reports of lipid bilayer formation below or close to the lipid transition temperature.<sup>29</sup> Seantier et al. studied the effect of deposition temperature on bilayer formation by tuning the  $T_m$  of the vesicles by mixing shorter-chain lipid 1,2-dimyristoyl-*sn*-glycero-3-phosphocholine (DMPC) with DPPC.<sup>29</sup> In this way, the  $T_m$  can be reduced from 42 °C (pure DPPC) to 33 °C (50:50) or 29 °C (70:30). Bilayer formation was accomplished for the latter two cases at 24 °C, which is between the pretransition temperature and the main lipid transition temperature of the mixtures. Due to slow adsorption kinetics for the 50:50 sample (this was done without continuous flow), Seantier et al.<sup>29</sup> assumed that it was not possible to form SLBs from mixtures of higher DPPC content (and pure DPPC). Our results clearly show that it is possible to form DPPC bilayers below the  $T_m$  if continuous flow is used to ensure efficient mass transfer to the surface. In this case, the kinetics and coverage are similar to those for deposition above the  $T_m$ . (See QCM-D traces in Figure 1A and the fast bilayer formation visualized by AFM in Figure 1B.) For SLBs deposited above the main transition, the lipid molecules take up 36% more volume than in the gel phase, and thus subsequent cooling led to shrinking of the bilayer area as seen in our neutron reflection data as a decrease in surface coverage from  $91 \pm 3$  to  $68 \pm 3$  v/v% after cooling (sample 1, Table 1). In contrast, the bilayer deposited at 25 °C (sample 2) had a higher coverage ( $87 \pm 3$  v/v%), which was similar to the fluid membrane at 50 °C in sample 1 ( $91 \pm 3$  v/v%). Such cooling-induced defects have previously been visualized directly by temperature-controlled AFM imaging.<sup>30</sup>

In experiments that are carried out using instruments that are highly sensitive to the wet mass such as QCM-D, it is very likely that the signals from bilayer formation are completely masked by the attachment of vesicles on top of the bilayer, which seems to be particularly prominent at temperatures below the lipid  $T_m$ . Thus, even though QCM-D data indicates that a vesicular

layer is formed, this does not exclude that a full bilayer membrane can exist below.

## OUTLOOK

While QCM-D is very sensitive to the presence of vesicles, neutron reflection probes the bilayer composition and structure, and AFM can provide the local topological picture in terms of lateral organization. By using continuous flow mode AFM,<sup>4</sup> all steps of bilayer formation including vesicle attachment are captured and visualized. The combination of these techniques clearly shows that DPPC SLBs can be formed regardless of the temperature of deposition, but subsequent cooling effects on the final structure need to be taken into account. We have demonstrated this for the simple system composed of DPPC, but it is likely to be equally true for more complex membranes formed from charged lipids or those extracted from bacteria.<sup>17,19,20</sup> It should be noted that, in general, the nature of the lipids and the surface determine the outcome of vesicle fusion, in addition to the solution pH, ionic strength, and presence of divalent cations. It can thus be expected that no universal recipe for bilayer formation above or below the lipid  $T_m$  can be found as such. However, we have recently succeeded in forming bilayers of total lipid extracts from *E. coli*, despite their complex lipid composition, demonstrating that the solution conditions are equally important to temperature in successful SLB formation. These results are currently being prepared for publication.

## ASSOCIATED CONTENT

### Supporting Information

QCM-D traces for the deposition of DPPC bilayers in buffer and in pure water at 25 and at 50 °C. Additional information on neutron reflection measurements, fitting procedures, and models. SAXS data of multilamellar DPPC vesicles used to obtain the lamellar repeat distance. This material is available free of charge via the Internet at <http://pubs.acs.org>.

## AUTHOR INFORMATION

### Corresponding Authors

\*E-mail: [tania@nano.ku.dk](mailto:tania@nano.ku.dk).

\*E-mail: [marite.cardenas@mah.se](mailto:marite.cardenas@mah.se); [cardenas@nano.ku.dk](mailto:cardenas@nano.ku.dk).

### Notes

The authors declare no competing financial interest.

## ACKNOWLEDGMENTS

We thank Pierre-Yves Chapuis and Kell Mortensen for access to the SAXS instrument. M.C. gratefully acknowledges financial support from the Center for Synthetic Biology at Copenhagen University funded by the UNIK research initiative of the Danish Ministry of Science, Technology and Innovation, the DANSCATT Centre funded by the Danish government, and the Swedish Research Council. T.K.L. thanks the European Spallation Source, ESS AB for funding her Ph.D. We thank neutron scattering facilities Institut Laue Langevin (Grenoble, France) and ISIS (Didcot, U.K.) for allocated beam time and Robert Barker (ILL) and Maximilian Skoda (ISIS) for local support.

## REFERENCES

- (1) Eeman, M.; Deleu, M. From biological membranes to biomimetic model membranes. *Biotechnol. Agron. Soc.* **2010**, *14*, 719–736.

- (2) Balashev, K.; John DiNardo, N.; Callisen, T. H.; Svendsen, A.; Bjornholm, T. Atomic force microscope visualization of lipid bilayer degradation due to action of phospholipase A2 and Humicola lanuginosa lipase. *Biochim. Biophys. Acta* **2007**, *1768*, 90–99.
- (3) Fernandez, D. I.; Le Brun, A. P.; Lee, T. H.; Bansal, P.; Aguilar, M. I.; James, M.; Separovic, F. Structural effects of the antimicrobial peptide maculatin 1.1 on supported lipid bilayers. *Eur. Biophys. J.* **2013**, *42*, 47–59.
- (4) Lind, T. K.; Zielinska, P.; Wacklin, H. P.; Urbanczyk-Lipkowska, Z.; Cardenas, M. Continuous flow atomic force microscopy imaging reveals fluidity and time-dependent interactions of antimicrobial dendrimer with model lipid membranes. *ACS Nano* **2014**, *8*, 396–408.
- (5) Richter, R.; Mukhopadhyay, A.; Brisson, A. Pathways of lipid vesicle deposition on solid surfaces: A combined QCM-D and AFM study. *Biophys. J.* **2003**, *85*, 3035–3047.
- (6) Ollivon, M.; Lesieur, S.; Grabielle-Madelmont, C.; Paternostre, M. Vesicle reconstitution from lipid-detergent mixed micelles. *Biochim. Biophys. Acta* **2000**, *1508*, 34–50.
- (7) Kataoka-Hamai, C.; Higuchi, M.; Iwai, H.; Miyahara, Y. Detergent-mediated formation of polymer-supported phospholipid bilayers. *Langmuir* **2010**, *26*, 14600–14605.
- (8) Blodgett, K. B. Films built by depositing successive monomolecular layers on a solid surface. *J. Am. Chem. Soc.* **1935**, *57*, 1007–1022.
- (9) Richter, R. P.; Brisson, A. R. Following the formation of supported lipid bilayers on mica: a study combining AFM, QCM-D, and ellipsometry. *Biophys. J.* **2005**, *88*, 3422–3433.
- (10) Richter, R. P.; Berat, R.; Brisson, A. R. Formation of solid-supported lipid bilayers: An integrated view. *Langmuir* **2006**, *22*, 3497–3505.
- (11) Åkesson, A.; Lind, T.; Ehrlich, N.; Stamou, D.; Wacklin, H. P.; Cárdenas, M. Composition and structure of mixed phospholipid supported bilayers formed by POPC and DPPC. *Soft Matter* **2012**, *8*, 5658–5665.
- (12) Wacklin, H. P. Composition and Asymmetry in Supported Membranes Formed by Vesicle Fusion. *Langmuir* **2011**, *27*, 7698–7707.
- (13) Wacklin, H. P.; Thomas, R. K. Spontaneous formation of asymmetric lipid bilayers by adsorption of vesicles. *Langmuir* **2007**, *23*, 7644–7651.
- (14) Bernchou, U.; Brewer, J.; Midtby, H. S.; Ipsen, J. H.; Bagatolli, L. A.; Simonsen, A. C. Texture of lipid bilayer domains. *J. Am. Chem. Soc.* **2009**, *131*, 14130–14131.
- (15) Andrecka, J.; Spillane, K. M.; Ortega-Arroyo, J.; Kukura, P. Direct observation and control of supported lipid bilayer formation with interferometric scattering microscopy. *ACS Nano* **2013**, *7*, 10662–10670.
- (16) Seantier, B.; Breffa, C.; Félix, O.; Decher, G. Dissipation-Enhanced Quartz Crystal Microbalance Studies on the Experimental Parameters Controlling the Formation of Supported Lipid Bilayers. *J. Phys. Chem. B* **2005**, *109*, 21755–21765.
- (17) Dodd, C. E.; Johnson, B. R. G.; Jeuken, L. J. C.; Bugg, T. D. H.; Bushby, R. J.; Evans, S. D. Native E. coli inner membrane incorporation in solid-supported lipid bilayer membranes. *Biointerphases* **2008**, *3*, FA59–FA67.
- (18) Tian, C.; Tetreault, E.; Huang, C. K.; Dahms, T. E. Electrostatic interactions of colicin E1 with the surface of Escherichia coli total lipid. *Biochim. Biophys. Acta* **2006**, *1758*, 693–701.
- (19) Domenech, O.; Merino-Montero, S.; Montero, M. T.; Hernandez-Borrell, J. Surface planar bilayers of phospholipids used in protein membrane reconstitution: an atomic force microscopy study. *Colloids Surf., B* **2006**, *47*, 102–106.
- (20) Merino, S.; Domenech, O.; Diez, I.; Sanz, F.; Vinas, M.; Montero, M. T.; Hernandez-Borrell, J. Effects of ciprofloxacin on Escherichia coli lipid bilayers: An atomic force microscopy study. *Langmuir* **2003**, *19*, 6922–6927.
- (21) Cho, N.-J.; Frank, C. W.; Kasemo, B.; Höök, F. Quartz crystal microbalance with dissipation monitoring of supported lipid bilayers on various substrates. *Nat. Protoc.* **2010**, *5*, 1096–1106.
- (22) Campbell, R. A.; Wacklin, H. P.; Sutton, I.; Cubitt, R.; Fragneto, G. FIGARO: The new horizontal neutron reflectometer at the ILL. *Eur. Phys. J. Plus* **2011**, *126*, 107.
- (23) Cubitt, R.; Fragneto, G. D17: the new reflectometer at the ILL. *Appl. Phys. A: Mater. Sci. Process.* **2002**, *74*, S329–S331.
- (24) Vacklin, H. P.; Tiberg, F.; Fragneto, G.; Thomas, R. K. Composition of supported model membranes determined by neutron reflection. *Langmuir* **2005**, *21*, 2827–2837.
- (25) Nelson, A. Co-refinement of multiple-contrast neutron/X-ray reflectivity data using MOTOFIT. *J. Appl. Crystallogr.* **2006**, *39*, 273–276.
- (26) Reimhult, E.; Hook, F.; Kasemo, B. Intact vesicle adsorption and supported biomembrane formation from vesicles in solution: Influence of surface chemistry, vesicle size, temperature, and osmotic pressure. *Langmuir* **2003**, *19*, 1681–1691.
- (27) Nagle, J. F.; Tristram-Nagle, S. Structure of lipid bilayers. *Biochim. Biophys. Acta* **2000**, *1469*, 159–195.
- (28) Armen, R. S.; Uitto, O. D.; Feller, S. E. Phospholipid component volumes: Determination and application to bilayer structure calculations. *Biophys. J.* **1998**, *75*, 734–744.
- (29) Seantier, B.; Breffa, C.; Félix, O.; Decher, G. In situ investigations of the formation of mixed supported lipid bilayers close to the phase transition temperature. *Nano Lett.* **2004**, *4*, 5–10.
- (30) Leonenko, Z. V.; Finot, E.; Ma, H.; Dahms, T. E. S.; Cramb, D. T. Investigation of temperature-induced phase transitions in DOPC and DPPC phospholipid bilayers using temperature-controlled scanning force microscopy. *Biophys. J.* **2004**, *86*, 3783–3793.